

**Surface Ultrastructure in Developmental Stages of  
*Spirometra erinaceieuropaei* (Rudolphi, 1819) Mueller, 1937  
(Cestoda, Pseudophyllidea)**

TETSUYA OKINO

*Department of Parasitology, Kawasaki Medical School,  
577, Matsushima, Kurashiki 701-01, Japan.*

(Accepted March 22, 1996)

**Abstract**

The external morphology of all developmental stages (egg, coracidium, oncosphere, proceroid, plerocercoid and adult worm) of *Spirometra erinaceieuropaei* (Rudolphi, 1819) Mueller, 1937, was studied by scanning electron microscopy (SEM). The results obtained are summarized as follows: 1) The egg-shell had scattered deep pits on the surface and the pits varied in size from small to fairly large. 2) The surface of free-living coracidium was covered with long cilia and short projections. 3) When the oncosphere transformed into the proceroid, the projections on its surface changed in size and shape to conoid microtriches except the cercomer. 4) The thorn-shaped microtriches were observed only around a frontal pit of fully developed proceroid to early stage of plerocercoid. 5) Microtriches on the body surface in plerocercoid stage were conoid. 6) Filamentous microtriches were restricted to the surface of scolex from 7-day-old plerocercoid to adult worm. 7) In adult stage, digitiform microtriches were observed from neck region to gravid proglottides. 8) Many papillae around the genital atrium of mature proglottides appeared right after it formed. 9) Short digitiform microtriches on the surface of distal end and conoid microtriches on the proximal region of the cirrus were observed.

**Key words:** *Spirometra erinaceieuropaei*; developmental stages; surface ultrastructure; microtriches; SEM; Cestoda.

**Introduction**

Whole surface of cestodes is covered with numerous microtriches. Principal function of the microtrich is to absorb nutrient and protect the body from host immune response (Lee, 1972; Lumsden, 1975). Life cycle of *Spirometra erinaceieuropaei* involves egg, free-living coracidium, proceroid which develops in the hemocoel of copepods, plerocercoid which develops in numerous kinds of cold- and warm-blooded vertebrates except fishes, and adult worm which develops in small intestine of canine and feline families. The microtriches of the cestode change from conoid to digitiform through different stages from the proceroid to the adult (Bråten, 1968a, b; Grammeltvedt, 1973; Lumsden

*et al.*, 1974; Yazaki *et al.*, 1990), and structure and dimension of the microtriches vary in different regions of the body surface (Thompson *et al.*, 1980, 1982). Although Yamane *et al.* (1974, 1976a, b) previously described the surface topography of *S. erinacei*, accurate dates after infection is not clear, furthermore, full description of all developmental stages of worm has not been available.

The presence of pits on the egg-shell surface has been reported in pseudophyllidean cestodes (Hilliard, 1972; Ishii, 1972; Maejima *et al.*, 1983; Yamane *et al.*, 1976b). However, the pits of *S. erinaceieuropaei* eggs are much varied in size, pattern and arrangement, and the characteristics of the egg-shell of this species have not entirely been clarified.

In the present paper, the author reveals surface ultrastructure of all developmental stages of *S. erinaceieuropaei* by SEM to investigate the fine structural changes occurring with the transition of eggs to adult worms.

## Materials and Methods

### Eggs and coracidia

Plerocercoid larvae of *Spirometra erinacei-europaei* were obtained from the striped snake, *Elaphe quadrivirgata* captured in Okayama Prefecture, Japan. Three to 5 plerocercoids from the host snake were orally given to dogs ranging from 5 to 10 kg in weight. Eggs laid in physiological saline by a 20-day-old adult were used for SEM observations. The eggs for culture were collected from dog's feces at about 40 days postinfection (PI). The feces from the infected dogs were dissolved in tap water, and the eggs were collected by sieving fecal suspension. These eggs were smeared on a filter paper and incubated for 10 days at 25°C by the filter paper culture method of Harada and Mori (1955). To obtain coracidia the embryonated eggs were exposed under the sunlight or cold temperature (4°C).

### Oncospheres and procercooids

The fresh-water copepod, *Mesocyclops leuckarti* used for feeding experiments were collected from an irrigation canal in Kurashiki City. The liberated coracidia were exposed to copepods (about 50 coracidia per copepod in a Petri dish). The infected copepods were maintained in a glassware containing 2l of filtered canal water at 20°C added with rice straw infusion. Oncospheres were artificially removed the coracidial sheath in Medium 199. Procercooids were obtained from the infected copepods at 1–20 days PI.

### Plerocercoids

Female ICR mice were ingested the copepods containing 20-day-old procercooids, and plerocercoids were obtained from the infected mice at 5, 7 and 14 days PI. Each of 3 mice was orally given 10 plerocercoids from the host snake and autopsied after 90 min, 48 hrs and 5 days, respectively. The stretching of the plerocercoid head was done in ethanol-physiological saline solution (10% ethanol in physiological saline) and chloretone-physiological saline solution (0.1% chloretone in physiological saline) as described by Okino and Hatsushika (1987).

### Adult worms

Each of 4 dogs was orally given 100, 10, 4 and 5 plerocercoids from the host snakes and autopsied respectively at 1, 5, 110 and 173 days PI. Adult worms were recovered from intestines of the infected dogs.

### SEM observations

The specimens were fixed for 2 hrs with 2.5% glutaraldehyde in 0.05 M phosphate buffer (pH 7.4) at room temperature or at 4°C. Coracidia and procercooids were placed on a filter paper coated with platinum-palladium to facilitate handling. These specimens were postfixed for 1.5 hrs with 1% osmium tetroxide in 0.15 M phosphate buffer (pH 7.4) at 4°C. Adult worms of 110 and 173 days PI were stained with 2% tannic acid overnight and 1% osmium tetroxide for 1 hr to enhance conductivity. The specimens were then dehydrated through a graded series of ethanol, dried in a CO<sub>2</sub> critical-point apparatus or freeze-dried with the t-butyl alcohol using a freeze-drying device (JFD-300, JEOL Ltd.), coated with platinum-palladium, and studied with a Hitachi S-570 SEM.

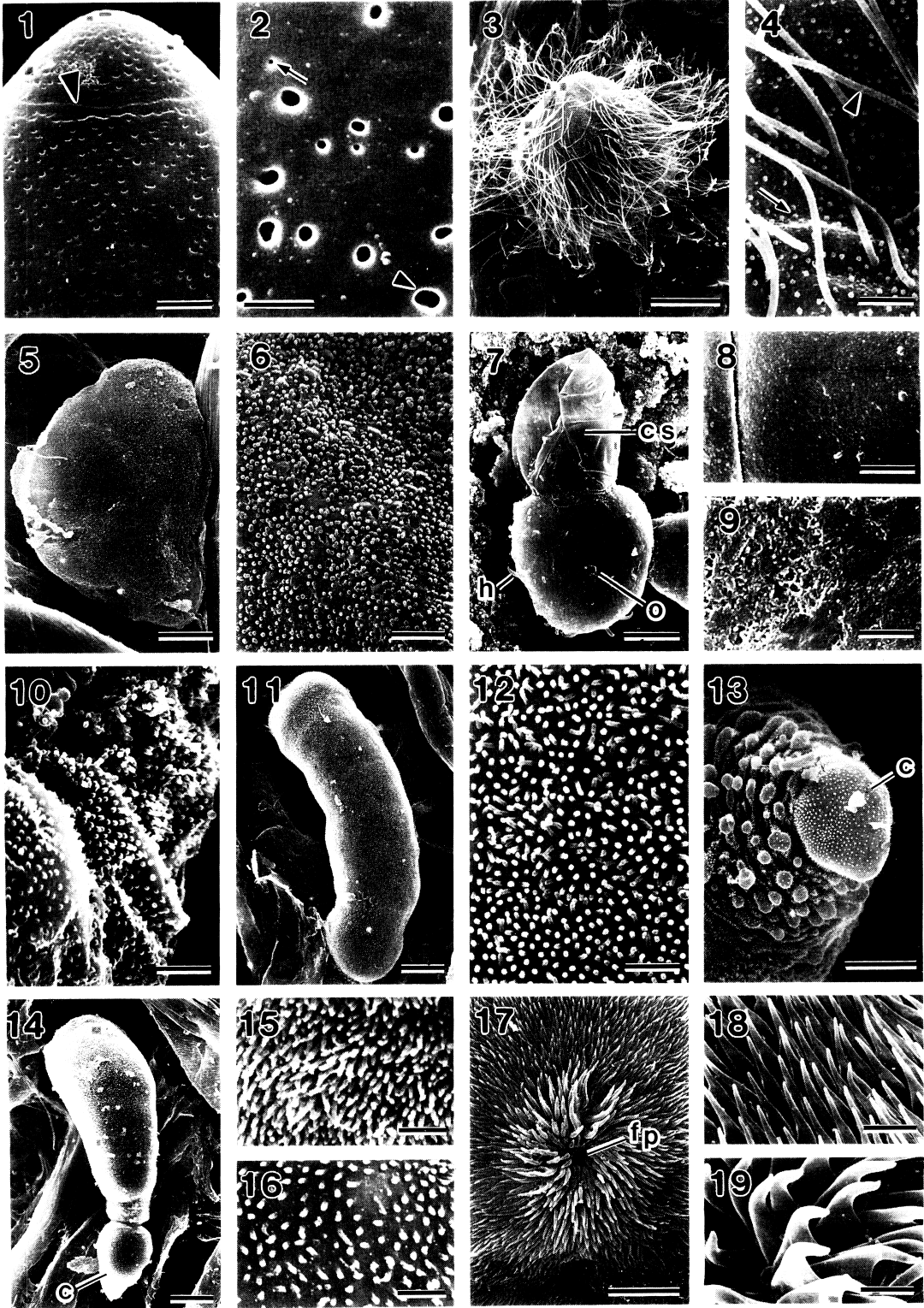
## Results

### Eggs and free-living coracidia

The eggs were football-shaped; the surface of the egg-shell had scattered deep pits and the opercular suture (Fig. 1). Central surfaces of 10 eggs were examined and the size of 279 pits were measured. Number of the pits ranged from 19 to 33 per 25 square  $\mu\text{ms}$  in surface area. The pits varied from 25 to 370 nm in diameter; the surface among these pits was smooth (Fig. 2). The liberated coracidium was spherical in shape with numerous cilia (Fig. 3). Surface of the coracidium was covered with long cilia (0.2  $\mu\text{m}$  in diameter) and club-like projections (0.1  $\mu\text{m}$  in diameter) (Fig. 4).

### Larvae removed from the 1st intermediate host

The coracidia immediately after infection to the copepods lost their cilia in the copepod gut (Fig. 5), the surface of the coracidia was covered with numerous club-like projections (Fig. 6). The coracidial sheath was shed in the gut of copepod. This process has also been accomplished in Medium 199 *in vitro*.



When oncosphere was shedding the coracidial sheath in Medium 199, the sheath was reversed and the hooks were protruded (Fig. 7). The inner surface of the coracidial sheath was smooth (Fig. 8), whereas the surface of oncosphere was rough and no projection or microtrich was recognized (Fig. 9). Numerous short projections ( $0.2\ \mu\text{m}$  in length and  $0.1\ \mu\text{m}$  in diameter) were observed on the surface of the larvae at 3 days PI (Fig. 10). The larvae at 5 days PI were club-shaped with no cercomer (Fig. 11), and the surface was covered with numerous projections ( $0.3\ \mu\text{m}$  in length and  $0.1\ \mu\text{m}$  in diameter) (Fig. 12). The cercomer formation occurred at the posterior end of the young proceroid at 10 days PI (Fig. 13). The transitional area from the proceroid body to the cercomer was narrow and it was easily recognized at 10 days PI (Fig. 14). The body surface of proceroid was covered with numerous pointed projections (i.e., microtriches) (Fig. 15), but that of cercomer was covered with sparse short projections (Fig. 16). Frontal pit was observed at the most anterior end of fully developed proceroid at 20 days PI (Fig. 17). The body surface of proceroid of this stage was covered with conoid microtriches except the cercomer (Fig. 18), although entire circumference of the frontal pit was limited only to the thorn-shaped microtriches (Fig. 19).

#### *Larvae removed from the 2nd intermediate host*

A young plerocercoid removed from the mouse at 5 days PI was tongue-shaped, about  $450\ \mu\text{m}$  in length, showing the one end much sharper than the other side which lacked the cercomer existed in the proceroid stage (Fig. 20). Thorn-shaped microtriches were observed at the top of the young plerocercoid, which closely resembled the microtriches situated around the frontal pit of fully developed proceroids (Fig. 21). On the surface of an anterior part of the plerocercoid the conoid microtriches were observed (Fig. 22), but no microtrich was present on the surface behind a middle part of the plerocercoid (Fig. 23). The plerocercoids removed from the mouse at 7 days PI had contractile head and short tail, and body length was about 1.6 mm (Fig. 24). Filamentous microtriches were observed on the surface of an anterior end of the plerocercoids of this stage (Fig. 25). The surface of anterior part of the plerocercoid was covered with conoid microtriches (Fig. 26), and short microtriches were observed on the surface of posterior part of the plerocercoid (Fig. 27). The first sign of bothridia was observed at head region of plerocercoids removed from mouse muscle at 14 days PI (Fig. 28), dorsal and ventral bothridia were well-defined (Fig. 29). The microtriches around the frontal pit of the

Figs. 1–2 Egg laid by adult worm at 20 days PI.

Fig. 1 Surface of egg-shell showing scattered deep pits and the opercular suture (arrowhead). (Scale bar =  $3\ \mu\text{m}$ )

Fig. 2 Pits of central part of egg-shell. Note: small (arrow) to large (arrowhead) pits. (Scale bar =  $1\ \mu\text{m}$ )

Figs. 3–6 Coracidia.

Fig. 3 Liberated coracidium with numerous long cilia. (Scale bar =  $10\ \mu\text{m}$ )

Fig. 4 Surface of coracidium showing cilia (arrowhead) and club-like projections (arrow). (Scale bar =  $1\ \mu\text{m}$ )

Fig. 5 Coracidium lost the cilia, immediately after being fed to the copepod. (Scale bar =  $5\ \mu\text{m}$ )

Fig. 6 Enlarged view of the surface of coracidium showing numerous club-like projections. (Scale bar =  $1\ \mu\text{m}$ )

Figs. 7–9 Oncosphere.

Fig. 7 Oncosphere just removed the coracidial sheath (cs) in Medium 199. (Scale bar =  $10\ \mu\text{m}$ ) h: hook, o: oncosphere.

Fig. 8 Enlarged view of the inner smooth surface of the coracidial sheath. (Scale bar =  $1\ \mu\text{m}$ )

Fig. 9 Enlarged view of the rough surface of oncosphere. Note: no projection on the surface. (Scale bar =  $1\ \mu\text{m}$ )

Figs. 10–19 Larvae removed from the copepod hemocoels of the 1st intermediate host.

Fig. 10 Surface of a larva with numerous short projections at 3 days PI. (Scale bar =  $1\ \mu\text{m}$ )

Fig. 11 Whole body of a club-shaped larva with no cercomer at 5 days PI. (Scale bar =  $10\ \mu\text{m}$ )

Fig. 12 Surface of the larva showing numerous short projections. (Scale bar =  $1\ \mu\text{m}$ )

Fig. 13 Surface of a posterior end of young proceroid with cercomer (c) at 10 days PI. (Scale bar =  $5\ \mu\text{m}$ )

Fig. 14 Proceroid with cercomer (c) at 10 days PI. (Scale bar =  $10\ \mu\text{m}$ )

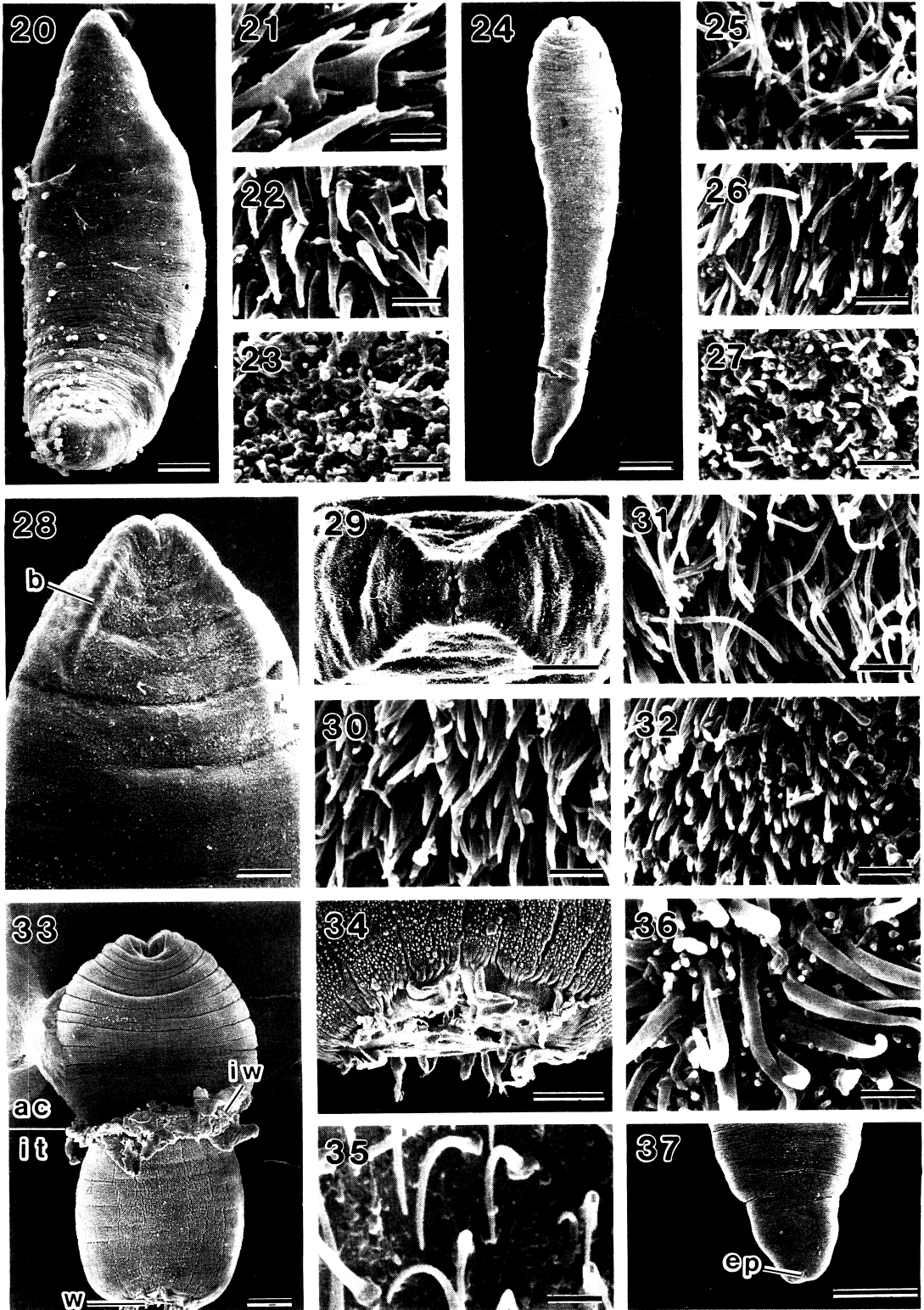
Fig. 15 Surface of the body of proceroid with numerous short microtriches. (Scale bar =  $1\ \mu\text{m}$ )

Fig. 16 Surface of the cercomer of proceroid with sparse short projections. (Scale bar =  $1\ \mu\text{m}$ )

Fig. 17 Apical view of fully developed proceroid at 20 days PI. (Scale bar =  $5\ \mu\text{m}$ ) fp: frontal pit.

Fig. 18 Conoid microtriches on the body surface of proceroid. (Scale bar =  $1\ \mu\text{m}$ )

Fig. 19 Thorn-shaped microtriches around the frontal pit of proceroid. (Scale bar =  $1\ \mu\text{m}$ )



plerocercoid were conoid (Fig. 30), and the microtriches on the bothria of it were filamentous (Fig. 31). Short conoid microtriches were observed on the posterior part of the plerocercoid (Fig. 32).

#### *Larvae removed from the paratenic host*

The plerocercoid shed the most posterior part of the body and only head of the larva penetrated into the intestinal wall of a paratenic host after oral ingestion. The plerocercoid just penetrating into the intestinal wall of the paratenic host was constricted at the middle part of body, and had the tegumentary wound portion on the surface of the caudal end (Fig. 33). Muscular contraction and twisted tegument were observed at the wound region (Fig. 34). Some remaining microtriches were observed on the thin tegument covered the wound portion (Fig. 35). Small microtriches were observed among large blade-like microtriches on the surface of the posterior end of plerocercoid at 48 hrs PI (Fig. 36). The plerocercoid healed the wound and the tail was regenerated at 5 days PI (Fig. 37).

#### *Adult worms recovered from the final host*

Scolex of early adult worm recovered from the infected dog at 24 hrs PI was spatular shape, and the scolex had the more developed bothridia than those

of the plerocercoid stage (Fig. 38). In apical view the scolex resembled a letter X because of its developed bothridia (Fig. 39), and frontal pit was clearly observed on apical end of the scolex (Fig. 40). Both short filamentous and conoid microtriches were observed around the frontal pit (Fig. 41), and the surfaces of bothria and bothridia were covered with filamentous microtriches (Fig. 42). Posterior portion of the early adult worm was round and no twisted tegument was observed (Fig. 43). The surface of the posterior portion was covered with conoid and short microtriches (Fig. 44). Scolex of young adult worm recovered from the infected dog at 5 days PI had well-developed bothridia and a frontal pit (Fig. 45), and microtriches around the frontal pit were both filamentous and conoid (Fig. 46). The surfaces of bothridia and bothria were covered with numerous filamentous microtriches (Fig. 47). Strobilization of the adult worm already began at 5 days PI (Fig. 48), and the surface of immature proglottid was covered with digitiform microtriches (Fig. 49). The scolex of fully developed adult worm at 110 days PI had more well-developed bothridia which shading bothria (Fig. 50). The number of proglottides of adult worm at 110 days PI was totally 1131 from the scolex to the terminal gravid proglottid. Slightly depressed geni-

---

Figs. 20–32 Larvae removed from the mouse tissue of the 2nd intermediate host.

Fig. 20 Whole body of a young plerocercoid at 5 days PI. (Scale bar = 50  $\mu$ m)

Fig. 21 Thorn-shaped microtriches around the frontal pit of plerocercoid. (Scale bar = 1  $\mu$ m)

Fig. 22 Conoid microtriches on the anterior part of plerocercoid. (Scale bar = 1  $\mu$ m)

Fig. 23 Surface of the middle part of plerocercoid. Note: no microtrich presents. (Scale bar = 1  $\mu$ m)

Fig. 24 Whole body of a plerocercoid at 7 days PI. (Scale bar = 200  $\mu$ m)

Fig. 25 Filamentous microtriches on the anterior end of plerocercoid. (Scale bar = 1  $\mu$ m)

Fig. 26 Conoid microtriches on the anterior part of plerocercoid. (Scale bar = 1  $\mu$ m)

Fig. 27 Short microtriches on the posterior part of plerocercoid. (Scale bar = 1  $\mu$ m)

Fig. 28 Head region of fully developed plerocercoid at 14 days PI. Note: first sign of bothridia. (Scale bar = 50  $\mu$ m) b: bothridium.

Fig. 29 Apical view of the anterior end of plerocercoid. Note: well-defined dorsal and ventral bothria. (Scale bar = 50  $\mu$ m)

Fig. 30 Conoid microtriches around the frontal pit of plerocercoid. (Scale bar = 1  $\mu$ m)

Fig. 31 Filamentous microtriches on the bothrium of plerocercoid. (Scale bar = 1  $\mu$ m)

Fig. 32 Short conoid microtriches on a posterior part of plerocercoid at 14 days PI. (Scale bar = 1  $\mu$ m)

Figs. 33–37 Larvae removed from mouse tissue of the paratenic host.

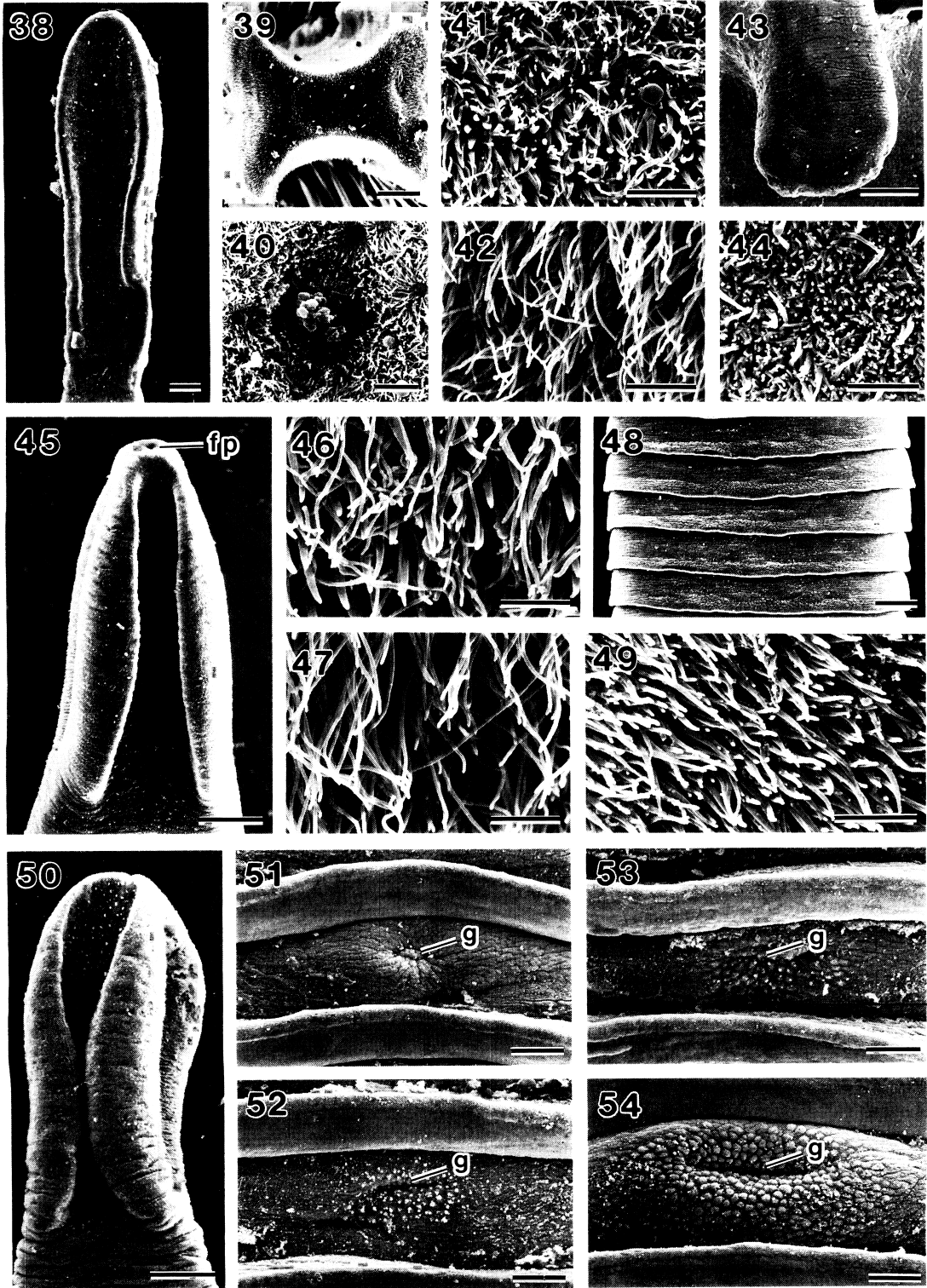
Fig. 33 A plerocercoid just penetrating intestinal wall (iw) of mouse at 90 min PI. Note: tegumentary wound (w) on a posterior end of plerocercoid. (Scale bar = 200  $\mu$ m) ac: abdominal cavity, it: intestinal tract.

Fig. 34 Enlarged view of the posterior end of plerocercoid with the tegumentary wound. Note: twisted tegument around wound. (Scale bar = 100  $\mu$ m)

Fig. 35 Remaining microtriches on thin tegument covered wound portion. (Scale bar = 1  $\mu$ m)

Fig. 36 Large blade-like and small microtriches on a posterior end of plerocercoid at 48 hrs PI. (Scale bar = 1  $\mu$ m)

Fig. 37 A posterior portion of plerocercoid with regenerated tail at 5 days PI. (Scale bar = 200  $\mu$ m) ep: excretory pore.



tal atrium appeared first on the surface of the central region of the 532nd proglottid posterior to scolex (Fig. 51), and depressed genital atrium (about 50  $\mu\text{m}$  in width) was observed on the surface of the central region of the 551st proglottid (Fig. 52). Slightly projected several tens papillae were found on the surface around the genital atrium of the central region of the 555th proglottid (Fig. 53). Numerous marked papillae were found on the surface around the genital atrium (about 100  $\mu\text{m}$  in width) of the central region of the 572nd mature proglottid (Fig. 54). Digitiform microtriches were observed on the surface of immature proglottid and this type of microtriches were usually observed on the surfaces of neck, immature, mature and gravid proglottides (Fig. 55). On the ventral surface of fully gravid proglottides, numerous papillae were seen. The surface of the papillae was covered with digitiform microtriches (Fig. 56). No papilla was observed on the dorsal surface of gravid proglottides and its surface was covered with digitiform microtriches which were more slightly slender than those of the immature proglottides (Fig. 57).

Most of the cirri were embedded in the genital atrium in gravid proglottides, though some cirri in gravid proglottides protruded above the surface. They were cone-shaped and the tip was round (Fig. 58). Short digitiform microtriches were observed on the distal end of the cirrus (Fig. 59), and the proximal

region of the cirrus was covered with the conoid microtriches (Fig. 60).

## Discussion

The materials used in the present study were obtained by the experimental infection in the laboratory, so that the accurate dates of PI are well-defined. With the use of experimental materials, detailed external feature of all developmental stages (egg, coracidium, oncosphere, proceroid, plerocercoid and adult worm) of *S. erinacei* was able to study by SEM.

The egg-shell of *S. erinacei* had deep pits on the surface ranging from 25–370 nm and the density of pits were 19 to 33 per 25 square  $\mu\text{m}$ s. In *S. erinacei*, Yamane *et al.* (1976b) described that shallow pits were sparsely distributed and Maejima *et al.* (1983) reported that the pits on the egg-shell surface showed a wide range of variety of size, shape and density, without actual measurements. Although Ishii (1972) reported that the size of pits ranged from 0.1 to 1.0  $\mu\text{m}$ , the measurements in the present study were smaller than his ones. The present study revealed that the existence of the pits with various size on the surface of each egg-shell is characteristic for *S. erinacei*.

The surface of coracidium had numerous long cilia and short projections. Yamane *et al.* (1976a)

---

Figs. 38–60 Adult worms recovered from small intestines of the infected dog.

Fig. 38 Scolex of early adult worm at 24 hrs PI. (Scale bar = 50  $\mu\text{m}$ )

Fig. 39 Apical view of the scolex. (Scale bar = 25  $\mu\text{m}$ )

Fig. 40 Enlarged view of the frontal pit. (Scale bar = 25  $\mu\text{m}$ )

Fig. 41 Short filamentous and conoid microtriches around the frontal pit. (Scale bar = 2  $\mu\text{m}$ )

Fig. 42 Filamentous microtriches on the surface of bothrium. (Scale bar = 2  $\mu\text{m}$ )

Fig. 43 Surface of a posterior portion of early adult worm at 24 hrs PI. Note: no twisted tegument presents. (Scale bar = 100  $\mu\text{m}$ )

Fig. 44 Enlarged view of the posterior surface, showing conoid and short microtriches. (Scale bar = 2  $\mu\text{m}$ )

Fig. 45 Scolex of young adult worm at 5 days PI. (Scale bar = 100  $\mu\text{m}$ ) fp: frontal pit.

Fig. 46 Filamentous and conoid microtriches around the frontal pit. (Scale bar = 2  $\mu\text{m}$ )

Fig. 47 Filamentous microtriches on the surface of bothridium. (Scale bar = 2  $\mu\text{m}$ )

Fig. 48 Immature proglottides of young adult worm at 5 days PI. (Scale bar = 100  $\mu\text{m}$ )

Fig. 49 Digitiform microtriches on the surface of immature proglottid. (Scale bar = 2  $\mu\text{m}$ )

Fig. 50 Scolex of fully developed adult worm at 110 days PI. (Scale bar = 100  $\mu\text{m}$ )

Fig. 51 Surface of a central region of mature proglottid (532nd proglottid posterior to scolex). Note: first sign of genital atrium (g). (Scale bar = 50  $\mu\text{m}$ )

Fig. 52 Depressed genital atrium (g) of mature proglottid (551st proglottid posterior to scolex). (Scale bar = 50  $\mu\text{m}$ )

Fig. 53 Surface of a central region of mature proglottid (555th proglottid posterior to scolex). Note: first sign of central papillae around genital atrium (g). (Scale bar = 50  $\mu\text{m}$ )

Fig. 54 Surface of a central region of mature proglottid (572nd proglottid posterior to scolex). Note: numerous marked papillae around genital atrium (g). (Scale bar = 50  $\mu\text{m}$ )



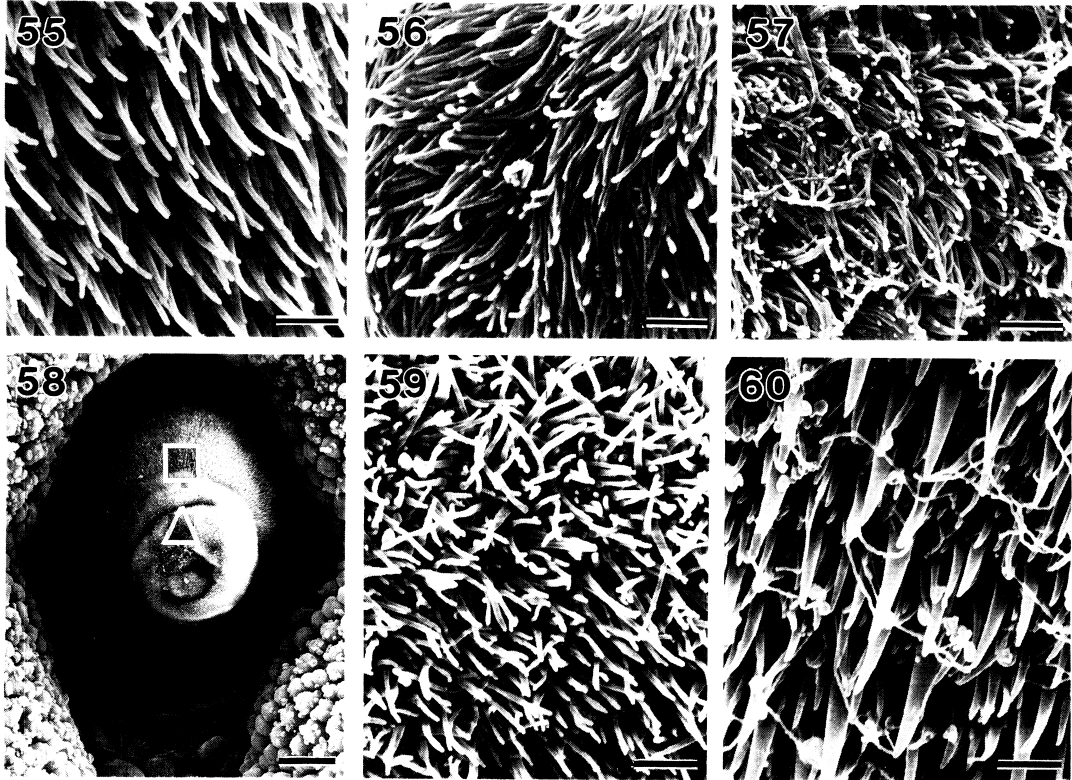


Fig. 55 Digitiform microtriches on a surface of immature proglottid of adult worm at 173 days PI. (Scale bar = 1  $\mu\text{m}$ )

Fig. 56 Digitiform microtriches on a papilla around genital atrium of the fully gravid proglottid. (Scale bar = 1  $\mu\text{m}$ )

Fig. 57 Digitiform microtriches on the dorsal surface of the fully gravid proglottid. (Scale bar = 1  $\mu\text{m}$ )

Fig. 58 Genital atrium of gravid proglottid of adult worm at 173 days PI. Note: protrudent cirrus and genital papillae. (Scale bar = 30  $\mu\text{m}$ )

Fig. 59 Enlarged view of triangular area indicated in Fig. 58 showing digitiform microtriches on the distal end of the cirrus. (Scale bar = 1  $\mu\text{m}$ )

Fig. 60 Enlarged view of square area indicated in Fig. 58 showing conoid microtriches on the proximal region of the cirrus. (Scale bar = 1  $\mu\text{m}$ )

reported that the coracidia of *S. erinacei* had the cilia and sting-like spines on the surface, but such spines were not observed in present study. In transmission electron microscope (TEM) studies on *S. mansonioides* coracidium, Lumsden *et al.* (1974) indicated that the outer layer of coracidium was a cytoplasmic syncytium whose free surface bore cilia and numerous club-like microvilli. It is conceivable that short projections are microvilli because these projections were very similar to their microvilli. The coracidial sheath was shed at time passing through the gut of copepod, and firstly cilia

of coracidium cast off, then the coracidial sheath was reversed in the gut of copepoda.

At the stages of early procercooids, the short projections were observed on the surface of young larvae at 3 to 5 days PI and the projections changed into microtriches on the body surface of procercooid except the cercomer at 5 to 10 days PI. In TEM studies on *Diphyllbothrium dendriticum* procercooids, Grammelvedt (1973) reported that the growing microvilli could be seen as early as 3 days PI and the tiny microtriches consisted of a base and a tip appeared at about 7 days PI. Lumsden *et al.*

(1974) also indicated that microvilli as the short digitiform projections were present at 24 to 72 hrs PI to copepod. The projections observed in the present study are considered to be microvilli because of similarity among three species in size and shape. In the polycephalic larvae of *Paricterotaenia paradoxa*, the microvilli were converted directly into microtriches (MacKinnon and Burt, 1984). Lumsden *et al.* (1974) described that the fate of the microvilli situated on the tegumental surface of the differentiating oncosphere is unknown. In *S. erinacei europaei*, the mechanism of transition of microvilli into microtriches is still not well-known.

In the fully developed proceroid at 20 days PI, conoid microtriches, thorn-shaped ones and microvilli were recognized on the surfaces of entire body, around the frontal pit and on the surface of cercomer, respectively. Thorn-shaped microtriches closely resembled those of *D. dendriticum* proceroid described by Grammeltvedt (1973). On the microvilli situated on the surface of cercomer, Grammeltvedt (1973) described that the fully developed proceroid have retained microvilli seen at the stage of earlier proceroid. Jarecka *et al.* (1981) also described that the cercomer was bound externally not by microtriches but by microvilli in *Triaenophorus nodulosus* and *Ligula intestinalis* proceroids. Following ingestion to 2nd intermediate host, the proceroid casts off its cercomer with microvilli, and only proceroid body with microtriches is able to grow thereafter. This suggests that the microvilli is not specifically adapted for protection and nutrient absorption in 2nd intermediate host.

In *S. erinacei europaei* filamentous microtriches were restricted to the scolex from 7-day-old plerocercoids to adult worms. In *Echinococcus granulosus*, filamentous microtriches were restricted to the scolex (Thompson *et al.*, 1982), and they concluded that these microtriches play an important functional role at interfacial region between rostellum of holdfast organ and host mucosa. It is assumed that filamentous microtriches play an important role for attaching to the host mucosa.

*S. erinacei europaei* plerocercoid had the tegumentary wound at its posterior end after shedding its tail in the intestine of a paratenic host. Okino and Hatsushika (1988) have previously reported external morphological changes of wound healing,

but detailed alteration of microtriches on the wound portion was not reported. In the present paper, small microtriches were observed among large blade-like microtriches on the surface of wound region at 48 hrs PI. Osaki (1990) reported that microtriches were stripped off the tegument in places during penetration into the intestinal wall of golden hamster, and small, fine and thread-like microtriches appeared on the stripped regions, although, these microtriches were not observed in present study. Osaki (1990) also reported that thin, short filamentous microtriches occasionally had electron-dense caps at 24 hrs PI, and these microtriches closely resembled the small microtriches. The detailed process of tegumentary wound healing is not quite understood.

Yamane *et al.* (1974) have found many papillae on the surface of central region of mature proglottides of *S. erinacei*. Okino and Hatsushika (1994) have reported that 3 types of clumps of papillae were present on the surface of fully gravid proglottides and the papillae were characteristic for *S. erinacei* adult. It can be useful as an index for cestode identification. Although they did not referred forming process of central clumps of papillae around genital atrium, the process can be summed as: appearance of the central clumps of papillae around genital atrium followed formation of depressed genital atrium for only 40 proglottides.

In *S. erinacei europaei*, most of the cirri were not everted and not observed on mature and gravid proglottides. The present study found that the surface of protrudent cirrus of adult *S. erinacei europaei* was covered with the conoid and digitiform microtriches. Beveridge and Smith (1985) reported that the cirrus of *Phyllobothrium vagans* was covered with blade-like, large and small filamentous microtriches. In *Cylindrotaenia hickmani*, the cirrus was lined by filamentous, hook-like and blade-like microtriches (Jones, 1989). It is probable that variation of microtriches shape may relate to the copulation process.

#### Acknowledgements

The author is indebted to Prof. R. Hatsushika for continuing guidance and keen advice. The author also wishes to thank Miss K. Matoba of our laboratory for her superb support. This study was supported by Research Project Grants (No. 2-707 and No. 3-508) from Kawasaki Medical School.

## References

- 1) Beveridge, I. and Smith, K. (1985): An ultrastructural study of the cirrus and vagina of *Phyllobothrium vagans* (Cestoda: Tetraphyllidea). *Z. Parasitenkd.*, 71, 609–616.
- 2) Bråten, T. (1968a): An electron microscope study of the tegument and associated structures of the procercoïd of *Diphyllobothrium latum* (L.). *Z. Parasitenkd.*, 30, 95–103.
- 3) Bråten, T. (1968b): The fine structure of the tegument of *Diphyllobothrium latum* (L.). A comparison of the plerocercoid and adult stages. *Z. Parasitenkd.*, 30, 104–112.
- 4) Grammeltvedt, A. F. (1973): Differentiation of the tegument and associated structures in *Diphyllobothrium dendriticum* Nitsch (1824) (Cestoda: Pseudophyllidea). An electron microscopical study. *Int. J. Parasitol.*, 3, 321–327.
- 5) Harada, Y. and Mori, O. (1955): A new method for culturing hook-worm. *Yonago Acta medica*, 1, 177–179.
- 6) Hilliard, D. K. (1972): Studies on the helminth fauna of Alaska. I. Observations on eggshell formation in some diphyllbothriid cestodes. *Can. J. Zool.*, 50, 585–592.
- 7) Ishii, Y. (1972): Morphology of helminth ova through the scanning electron microscope. *Fukuoka Acta medica*, 63, 419–431 (in Japanese).
- 8) Jarecka, L., Michajlow, W. and Burt, M. D. B. (1981): Comparative ultrastructure of cestode larvae and Janicki's cercomer theory. *Acta Parasit. Pol.*, 28, 65–72.
- 9) Jones, M. K. (1989): Ultrastructure of the cirrus pouch of *Cylindrotaenia hickmani* (Jones, 1985) (Cestoda, Nematotaeniidae). *Int. J. Parasitol.*, 19, 919–930.
- 10) Lee, D. L. (1972): The structure of the helminth cuticle. *Adv. Parasitol.*, 10, 347–379.
- 11) Lumsden, R. D. (1975): Surface ultrastructure and cytochemistry of parasitic helminths. *Exp. Parasitol.*, 37, 267–339.
- 12) Lumsden, R. D., Oaks, J. A. and Mueller, J. F. (1974): Brush border development in the tegument of the tapeworm, *Spirometra mansonioides*. *J. Parasitol.*, 60, 209–226.
- 13) MacKinnon, B. M. and Burt, M. D. B. (1984): The development of the tegument and cercomer of the polyccephalic larvae (cercoscolices) of *Paricterotaenia paradoxa* (Rudolphi, 1802) (Cestoda: Dilepididae) at the ultrastructural level. *Parasitology*, 88, 117–130.
- 14) Maejima, J., Yazaki, S. and Fukumoto, S. (1983): Morphological comparison of eggs between marine species and fresh-water species in diphyllbothriid cestodes. *Jpn. J. Parasitol.*, 32, 27–42 (in Japanese with English abstract).
- 15) Okino, T. and Hatsushika, R. (1987): Morphological study on the head of *Spirometra erinacei* plerocercoid by an improved stretching fixation technique. *Jpn. J. Parasitol.*, 36, 103–105 (in Japanese with English abstract).
- 16) Okino, T. and Hatsushika, R. (1988): Studies on tegumentary wound healing in *Spirometra erinacei* plerocercoids. *Jpn. J. Parasitol.*, 37, 209–213 (in Japanese with English abstract).
- 17) Okino, T. and Hatsushika, R. (1994): Ultrastructure studies on the papillae and the nonciliated sensory receptors of adult *Spirometra erinacei* (Cestoda, Pseudophyllidea). *Parasitol. Res.*, 80, 454–458.
- 18) Osaki, Y. (1990): Ultrastructural studies on the plerocercoid of *Spirometra erinacei* in experimental sparganosis. *Parasitol. Res.*, 76, 466–472.
- 19) Thompson, R. C. A., Hayton, A. R. and Jue Sue, L. P. (1980): An ultrastructural study of the microtriches of adult *Proteocephalus tidswelli* (Cestoda: Proteocephalidae). *Z. Parasitenkd.*, 64, 95–111.
- 20) Thompson, R. C. A., Houghton, A. and Zaman, V. (1982): A study of the microtriches of adult *Echinococcus granulosus* by scanning electron microscopy. *Int. J. Parasitol.*, 12, 579–583.
- 21) Yamane, Y., Maejima, J. and Kamo, H. (1974): Study of *Spirometra erinacei* (Rudolphi, 1819) Faust, Campbell and Kellogg, 1929 through scanning electron microscope. *Yonago Acta medica*, 18, 84–93.
- 22) Yamane, Y., Okada, N. and Seki, R. (1976a): Scanning electron microscopic observation of hatching in some diphyllbothriid cestodes. *Yonago Acta medica*, 20, 234–240.
- 23) Yamane, Y., Seki, R. and Okada, N. (1976b): Comparative observation on surface topography of teguments and eggshells of diphyllbothriid cestodes by scanning electron microscopy. *Yonago Acta medica*, 20, 55–65.
- 24) Yazaki, S., Fukumoto, S. and Maejima, J. (1990): Cytoskeletal construction and alteration of microtriches of *Diphyllobothrium hottai*, during early developmental stages. *Jpn. J. Parasitol.*, 39, 165–171.